



SRTTU

Journal of Computational and Applied Research
in Mechanical Engineering

jcarme.sru.ac.ir

JCARME

ISSN: 2228-7922

Research paper

Electrical resistance heating distribution on three dimensional Jeffrey radiating nanofluid flow past stretching surface

B. Malliswari^a, T. Poornima^b, P. Sreenivasulu^{c,*} and N. Bhaskar Reddy^a

^aDepartment of Mathematics, Sri Venkateswara University, Tirupati, A.P-517502, India.

^bFluid Dynamics Division, SAS, Vellore Institute of Technology, Vellore, T.N.-632014, India

^cDepartment of Science and Humanities, Sri Venkateswara Engineering college, Tirupati, A.P-517502., India.

Article info:

Article history:

Received: 15/06/2020
Revised: 02/07/2021
Accepted: 05/07/2021
Online: 10/07/2021

Keywords:

Magnetic field,
Non-linear radiation,
Ohmic heating,
Stretching surface,
Viscous dissipation,
Convective heat and mass flux.

*Corresponding author:

psreddysvu1@gmail.com

Abstract

This study emphasizes the upshots of non-linear radiation and electrical resistance heating on a three dimensional Jeffrey dissipating nanoflow in view of convective surface conditions. The initial set of nonlinear dimensional boundary layer equations are transformed into a system of ordinary differential equations with suitable similarity variables and then solved by shooting method using Mathematica software. For various representative quantities, the behavior of the momentum, energy and species diffusion along with engineering quantities near the surface are figured for different estimations of the fluid properties. The examination of the present outcomes has been made with the existing work which is in good agreement. This study helps in understanding that the heat transfer rate is predominant in the non-linear radiation compared to linear radiation. Jeffrey fluid model has the capacity of describing the stress relaxation property, that usually viscous fluid lags and this is exhibited clearly in the study. Shear stress descends as the fluid pertinent parameter ascends.

1. Introduction

Sir Isaac Newton is the father of the viscosity concept, stress-strain relation and originator of classical fluid dynamics. There are quite extensive fluids whose density differs with the tension inside (time-dependent) and such a

class is called non-Newtonian fluids. Various models were proposed to describe the nature of non-Newtonian fluids. Jeffrey's fluid model succeeded the other developed rheological models. Amongst them, Jeffrey-Hamel's fluid model is peculiar, as this fluid model at high surface shear stress ($>$ yield stress) degenerates

to Newtonian. This fluid model finds relation between relaxation to retardation time effects. Further, during circulation process, blood shows the qualities of Newtonian and non-Newtonian fluids. Major applications of rheological fluids are Slurries, physiological suspensions, molten plastic material, foams, food processing, geological materials, drilling muds, syrups, colloidal solutions, production, cosmetics, paints production and coating, etc.,. Sreenivasulu et al. [1] examined nanoparticles flux on bio-convective fluid. Ojjela et al. [2] examined within parallel permeable plates, the flow of Jeffrey fluid. Kahshan et al. [3] inspected the applications of this fluid on permeable channel.

Basing on its very important applications in the field of mechanical and designing procedures, the idea of stretching is more revolutionary. The overextension process gives a one way stretching, refining its mechanical properties. The cooling nature of the surface in the porous media depends on the fluid used and these situation is seen in textile industries, polymer processing, paper production, and manufacturing of the glass sheets. Flow past a stretching sheet in three dimensional was studied by Ariel [4]. MHD Casson fluid towards an elongated sheet was presented by Mahaboob and Kalidas [5]. Hussain et al. [6] analysed the second grade fluid taking the geometry as stretching surface. Singh et al. [7] investigated mass transpiration in MHD nonlinear flow along a porous extending surface. The influence of energy rise/fall past an extending surface was scrutinized by Ibrahim et al. [8].

Significant fields of science and engineering include magnetohydrodynamics as its part. Physiological fluids like blood have the conducting property; when it is under magnetic field it behaves appreciably as it helps in transporting drugs inside the body. For tumor treatments, drug targeting and treatment for cell death due to hyperthermia are all done by inserting the bio magnetic fluids in the blood stream. This bio-magnetic fluid produces a transverse magnetic field and supplies the drug at the desired place. Several studies have been published on influence of MHD on various fields [9-11]. Flow of magnetic field on imbibition

phenomenon was introduced by Gohil and Ramakanta [12]. Ramzan et al. [13] examined the entropy generation on bio-convective magnetic CNTs. MHD radiative UCM nanoflow under Joule heating effect was scrutinized by Sreenivasulu et al. [14].

Major industrial, research and public health sectors require the application of radiation. For tumor patients, the basic treatment is dispersion of the radiation which helps in destroying the damaged cells. For designing high thermal resistant equipment especially in space crafts, radiation role is indispensable. Radiation and chemical reaction effects on Peristaltic propulsion of Jeffrey nanofluid were inspected by Abbas et al. [15]. Hussain et al. [16] investigated the medium less heat transformation impact on viscoelastic nanofluid flow. Influence of thermal radiation in various fields has been studied by [17-19]. Radiation effect on MHD dusty fluid past a parabolic surface was investigated by Gnanaswara Reddy and Ferdows [20].

Conduction in the sheet is seen on one side and its adjacent is convection in the liquid. This physical occurrence is generally described as Newtonian condition and it is common nature in heat transfer surfaces, particularly in power plants run by thermal energy and gas turbines. Boundary conditions on both sides of the surface are not similar due to its spatial coordination. Negative sign in the condition indicates alternating energy flow near the wall. Hayat et al. [21] investigated the effect of variable thermal conductivity on radiating Jeffrey flow. Nayak et al. [22] have proposed the Newtonian condition effect on 3D slip MHD nanoflow embedded in porous medium. The influence of convective boundary on Bio-nanoflow along moving sheet was presented by Chan et al. [23].

Heat transfer problems encounter another important parameter, called viscous dissipation, the internal friction of the fluid having its major applications in engineering and science such as astrophysics, oceanography, meteorology, biomedicine, etc. Viscous dissipation turns the kinetic energy into internal friction energy. Viscous dissipation influence was initially investigated by Brickman [24].

Joule heating is another important aspect in heat transfer of hydrodynamic flows along with its applications such as electric heaters, electric fuses, soldering irons, electric cigarettes etc. Fillo [25] initiated the study of viscous dissipation combined with Ohmic heating. Hussain [26] studied the same combination on MHD Sisko fluids past a stretching cylinder; and Cattaneo-Christove heat flux past a Riga plate was investigated by Shamshuddin [27].

The primary intention of this investigation is exploring the Joule heating effect on 3D dissipating and radiating Jeffrey nanoflow sliding along extending sheet under usual heat and mass flux boundary conditions, as this topic has been paid little attention by researchers.

2. Formulation of flow model

Consider an incompressible, laminar, electrically conducting, steady, viscous three dimensional Jeffrey nanoflow along an extended surface. Newtonian boundary condition is incorporated. The flow is confined to positive z -axis and the sheet is stretched over xy -plane. A magnetic field of strength B (constant) is transversely. Since the fluid is conducting, electrical resistive heating is also distributed inside the fluid. The graphical abstract is shown in Fig. 1. Since the flow is laminar, Reynolds is much less than unity and hence the induced magnetic field is negligible. In this analysis, radiation has a non-linearized Rosseland assumption which is suitable for all ranges of temperature deviations (small or large).

Brownian motion, viscous dissipation and thermophoresis are also taken. Convective heating process takes place at the adjacent side of the surface and characterized by the h_f coefficient of heat transfer with the hot fluid temperature T_f . Under usual Boussinesq's approximation, Prandtl boundary layer obeying the situation taken from Hayat *et al.* [28] is given as:

$$\frac{\partial \bar{u}}{\partial x} + \frac{\partial \bar{v}}{\partial y} + \frac{\partial \bar{w}}{\partial z} = 0 \tag{1}$$

$$\frac{\bar{v}_f}{1 + \lambda} \frac{\partial^2 \bar{u}}{\partial z^2} - \frac{\bar{\sigma} \bar{B}^2}{\rho_f} \bar{u} = u \frac{\partial \bar{u}}{\partial x} + v \frac{\partial \bar{u}}{\partial y} + w \frac{\partial \bar{u}}{\partial z} \tag{2}$$

$$\frac{\bar{v}_f}{1 + \lambda} \frac{\partial^2 v}{\partial z^2} - \frac{\bar{\sigma} \bar{B}^2}{\rho_f} v = u \frac{\partial v}{\partial x} + v \frac{\partial v}{\partial y} + w \frac{\partial v}{\partial z} \tag{3}$$

$$\left. \begin{aligned} & \bar{\alpha}_f \frac{\partial^2 \bar{T}}{\partial z^2} - \frac{1}{(\rho C_p)_f} \frac{\partial \bar{q}_r}{\partial z} + \frac{\bar{\sigma} \bar{B}^2}{\rho_f C_p} (\bar{u}^2 + \bar{v}^2) \\ & \tau \left[\bar{D}_B \frac{\partial \bar{T}}{\partial z} \frac{\partial \bar{C}}{\partial z} + \frac{\bar{D}_T}{T_\infty} \left(\frac{\partial \bar{T}}{\partial z} \right)^2 \right] \\ & + \frac{2 \bar{\mu}_f}{\rho_f C_p} \left[\left(\frac{\partial \bar{u}}{\partial z} \right)^2 + \left(\frac{\partial \bar{v}}{\partial z} \right)^2 \right] \end{aligned} \right\} = u \frac{\partial \bar{T}}{\partial x} + v \frac{\partial \bar{T}}{\partial y} + w \frac{\partial \bar{T}}{\partial z} \tag{4}$$

$$\bar{D}_B \frac{\partial^2 \bar{C}}{\partial z^2} + \frac{\bar{D}_T}{T_\infty} \frac{\partial^2 \bar{T}}{\partial z^2} = u \frac{\partial \bar{C}}{\partial x} + v \frac{\partial \bar{C}}{\partial y} + w \frac{\partial \bar{C}}{\partial z} \tag{5}$$

The constraints for the flow field are as below:

$$\left. \begin{aligned} & \bar{u} = \bar{u}_w, \bar{v} = \bar{v}_w, \bar{w} = 0, \\ & -\bar{k}_f \left(\frac{\partial \bar{T}}{\partial z} \right) = \bar{h}_f (\bar{T}_f - \bar{T}), \\ & -\bar{D}_B \left(\frac{\partial \bar{C}}{\partial z} \right) = \bar{h}_g (\bar{C}_f - \bar{C}) \end{aligned} \right\} \text{at } \bar{z} = 0 \tag{6}$$

$$\bar{u} \rightarrow 0, \bar{v} \rightarrow 0, \bar{T} \rightarrow \bar{T}_\infty, \bar{C} \rightarrow \bar{C}_\infty \text{ as } \bar{z} \rightarrow \infty$$

where \bar{C} -nanoparticle volume fraction (kg/m³), \bar{T} -energy (K), $\bar{x}, \bar{y}, \bar{z}$ -cartesian coordinates, $\bar{u}, \bar{v}, \bar{w}$ - velocity components (m/s), \bar{u}_w, \bar{v}_w - stretching velocities (m/s), \bar{k}_f - heat conductance (W.m⁻¹.K⁻¹), \bar{B}_0 -Magnetic field strength (Tesla), \bar{h}_f -Convective heat transfer, \bar{k}_e - averaging absorption coefficient, \bar{p} - pressure (Pa), \bar{q}_r -heat flux due to radiation(W/m²), $\rho \bar{C}_p$ -heat capacitance (J/(kg.K)), \bar{D}_B -mass diffusivity Coefficient , \bar{D}_T - thermophoresis parameter, $\bar{\sigma}$ - specific conductance(S/m), $\bar{\sigma}_s$ -Boltzmann constant (W/m². K⁻⁴), $\bar{\nu}$ -kinematic viscosity (m²/s), $\bar{\rho}$ -density (kg/m³), $\bar{\alpha}$ - thermal

diffusivity (m²/s), $\bar{\mu}$ -dynamic viscosity (Pa.s) and the suffices f, ∞ represents the parameters inside the nanofluid and in quiescent flow.

The above situation finds applications in the enhanced thermal and mass transfer, industrial processes, drug manufacture, transportation, house hold appliances, and chemical engineering.

The non-linear radiation term is $\bar{q}_r = -\frac{4}{3} \frac{\bar{\sigma}_s}{k_e} \frac{\partial \bar{T}^4}{\partial y}$. However the present study is

focused highly on dense fluids, \bar{T}^4 can be expanded about T_∞ and considering the first order term and leaving the higher orders as $4\bar{T}_\infty^3\bar{T} - 3\bar{T}_\infty^4$, as the energy variation inside the fluid is small. In view of the above expressions, energy equation turns to the form:

$$\left. \begin{aligned} & \frac{\bar{k}_f}{\bar{\rho}_f \bar{C}_p f} \frac{\partial}{\partial \bar{z}} \left\{ \left(1 + \frac{16\bar{\sigma}_s}{3k_e \bar{k}_f} \bar{T}^3 \right) \frac{\partial \bar{T}}{\partial \bar{z}} \right\} + \frac{\bar{\sigma} \bar{B}^2}{\bar{\rho}_f \bar{C}_p f} (\bar{u}^2 + \bar{v}^2) \\ & + \tau \left[\frac{\bar{D}_B}{\bar{D}_B} \frac{\partial \bar{T}}{\partial \bar{z}} \frac{\partial \bar{C}}{\partial \bar{z}} + \frac{\bar{D}_T}{\bar{T}_\infty} \left(\frac{\partial \bar{T}}{\partial \bar{z}} \right)^2 \right] + \frac{2\bar{\mu}_f}{\bar{\rho}_f \bar{C}_p f} \left[\left(\frac{\partial \bar{u}}{\partial \bar{z}} \right)^2 + \left(\frac{\partial \bar{v}}{\partial \bar{z}} \right)^2 \right] \end{aligned} \right\} \\ = \bar{u} \frac{\partial \bar{T}}{\partial \bar{x}} + \bar{v} \frac{\partial \bar{T}}{\partial \bar{y}} + \bar{w} \frac{\partial \bar{T}}{\partial \bar{z}} \quad (7)$$

Introducing similarity transformations to the turn the boundary layer equations to:

$$\begin{aligned} \bar{u} &= a\bar{x}f', \quad \bar{v} = a\bar{y}g', \quad \bar{w} = -\sqrt{a\bar{v}}(g(\eta) + f(\eta)), \\ \eta &= \sqrt{\frac{a}{\nu_f}} \bar{z}, \quad \theta(\eta) = \frac{\bar{T} - \bar{T}_\infty}{\bar{T}_f - \bar{T}_\infty}, \quad \phi(\eta) = \frac{\bar{C} - \bar{C}_\infty}{\bar{C}_f - \bar{C}_\infty}, \\ M &= \frac{\bar{\sigma} \bar{B}_0^2}{\bar{\rho}_f a}, \quad Pr = \frac{\bar{\nu}_f}{\alpha_f}, \quad Nb = \frac{\tau \bar{D}_B (\bar{C}_w - \bar{C}_\infty)}{\bar{\nu}_f}, \\ Nt &= \frac{\tau \bar{D}_T (\bar{T}_f - \bar{T}_\infty)}{\bar{T}_\infty \bar{\nu}_f}, \quad Ec_x = \frac{\bar{u}_w^2}{Cp_f (\bar{T}_f - \bar{T}_\infty)}, \\ Ec_y &= \frac{\bar{v}_w^2}{Cp_f (\bar{T}_f - \bar{T}_\infty)}, \quad Le = \frac{\bar{\nu}_f}{D_B}, \quad \gamma = \frac{\bar{h}_f}{k_f} \sqrt{\frac{\bar{\nu}_f}{a}}, \\ \delta &= \frac{\bar{h}_f}{k_f} \sqrt{\frac{\bar{\nu}_f}{a}}, \quad Re_x = \frac{\bar{u}_w \bar{x}}{\bar{\nu}_f}, \quad Re_y = \frac{\bar{v}_w}{\bar{\nu}_f}, \quad R = \frac{16\bar{\sigma}_s \bar{T}_\infty^3}{3k_e k_f} \end{aligned} \quad (8)$$

Using Eq. (8), Eqs. (2,3,5,6 and 7) takes the non-dimensional structure as:

$$f''' = (1 + \lambda)(f'^2 + Mf' - (f + g)f'') \quad (9)$$

$$g''' = (1 + \lambda)(g'^2 + Mg' - (f + g)g'') \quad (10)$$

$$\begin{aligned} & (1 + R(1 + (\theta_m - 1)\theta)^3 \theta')' = \\ & - Pr \left\{ \begin{aligned} & (f + g)\theta' + Ec_x [2f''^2 + Mf'^2] \\ & + Ec_y [2g''^2 + Mg'^2] + \\ & Nb\theta'\phi' + Nt\theta'^2 \end{aligned} \right\} \end{aligned} \quad (11)$$

$$\phi'' + Le(f + g)\phi' + \frac{Nt}{Nb} \theta'' = 0 \quad (12)$$

Non-dimensional constraints are:

$$\begin{aligned} & f'(0) = 1, f(0) = 0, g'(0) = c, g(0) = 0, \\ & \theta'(0) = -\gamma(1 - \theta(0)), \phi'(0) = -\delta(1 - \phi(0)) \\ & f'(\infty) \rightarrow 0, g'(\infty) \rightarrow 0, \theta(\infty) \rightarrow 0, \phi(\infty) \rightarrow 0 \end{aligned} \quad (13)$$

where, η -independent variable, f, g -velocity, θ -energy, θ_m -non-linear radiation, ϕ -nanoparticle volume fraction, c -stretch ratio, γ, δ -thermal and solutal Biot number, λ -Jeffrey fluid, Ec -Eckert number, Le -Lewis number, R -radiation parameter, Nb -Pedesis, Nt -thermophoresis parameters, respectively and Re -Reynolds number.

From the technological point of view, the wall shear stress for Jeffrey nanoflow along both directions, Nusselt number and Sherwood number in dimensional less structure and are defined as:

$$\begin{aligned} i) \tau_{zx} &= \frac{\mu}{1 + \lambda} \frac{\partial u}{\partial z} \Big|_{z=0}, \quad \tau_{zy} = \frac{\mu}{1 + \lambda} \frac{\partial v}{\partial z} \Big|_{z=0} \\ \Rightarrow C_{fx} Re_x^{1/2} &= \left(\frac{1}{1 + \lambda} \right) f''(0), \quad C_{fy} Re_y^{1/2} = \left(\frac{1}{1 + \lambda} \right) g''(0) \\ ii) Nu_x &= \frac{q_w x}{k(T_f - T_\infty)} \Rightarrow Nu_x Re_x^{-1/2} = -(1 + R(1 + (\theta_m - 1)\theta)^3) \theta'(0) \\ iii) Sh_x &= \frac{J_w x}{D_m(C_f - C_\infty)} \Rightarrow Sh_x Re_x^{-1/2} = -\phi'(0) \end{aligned} \quad (14)$$

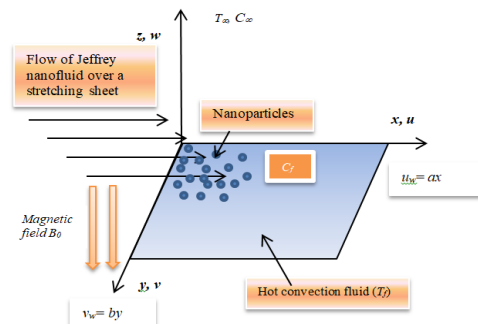


Fig. 1. Graphical abstract of the model.

3. Numerical exploration

The ordinary differential equations Eqs. (9-12) with associated conditions (13) of the Jeffry nanoflow model seem to be non-linear, when converted. Several numerical schemes are available, but shooting technique cum Runge-Kutta method has a great advantage, which has the fifth order truncation error. The algorithm of the method includes the following steps:

Step 1: Reducing the obtained non-linear differential equations to first order.i.e.:

$$\begin{aligned}
 f &= p_1; f' = p_1' = p_2; f'' = p_2' = p_3 \\
 p_3' &= -(1 + \lambda) \left\{ (y_1 + z_1) p_3 - p_2^2 - M p_2 \right\} \\
 g &= z_1; g' = z_1' = z_2; g'' = z_2' = z_3 \\
 z_3' &= -(1 + \lambda) \left\{ (y_1 + z_1) z_3 - z_2^2 - M z_2 \right\} \\
 \theta &= w_1; \theta' = w_1' = w_2 \\
 w_2' &= -\frac{\text{Pr}}{1 + R} \left(\begin{array}{l} (p_1 + z_1) w_2 + N b w_2 p_2 \\ + N t w_2^2 + E c_x \{ 2 p_3^2 + M p_2^2 \} \\ E c_y \{ 2 z_3^2 + M z_2^2 \} \end{array} \right) \\
 \phi &= y_1; \phi' = y_1' = y_2 \Rightarrow y_2' = -\left(L e (p_1 + z_1) y_2 + \frac{N t}{N b} w_2' \right) \\
 \phi &= y_1 \\
 \phi' &= y_1' = y_2 \Rightarrow y_2' = -\left(L e (p_1 + z_1) y_2 + \frac{N t}{N b} w_2' \right)
 \end{aligned}
 \tag{15}$$

The boundary conditions turn to be:

$$\begin{aligned}
 p_1(0) &= 0; p_2(0) = 1; z_1(0) = 0; z_2(0) = c; \\
 w_2(0) &= -\gamma(1 - w_1(0)); \\
 y_2(0) &= -\delta(1 - y_1(0)) \\
 p_2(\infty) &\rightarrow 0; z_2(\infty) \rightarrow 0; \\
 w_1(\infty) &\rightarrow 0; y_1(\infty) \rightarrow 0
 \end{aligned}
 \tag{16}$$

In Eq. (16), $p_3(0)$, $z_3(0)$, $w_2(0)$, $y_2(0)$ are to be determined.

Step 2: These are shot by taking suitable set of parameters.

Step 3: Choose initial values for $p_3(0)$, $z_3(0)$, $w_2(0)$, $y_2(0)$.

Step 4: Applying shooting technique, the values of unknown parameters are computed.

Step 5: The computed values are finalized if $|computed - initial| < 10^{-6}$ i.e., the difference between the initial and newly calculated values of $y_2(\infty)$, $z_2(\infty)$, $w_1(\infty)$ and $p_1(\infty)$ is absolutely less than 10^{-6} .

Step 6: If $|computed - initial| > 10^{-6}$, then initial approximations are to be modified again for different set of physical parameters. This process is repeated until desired convergence.

Step 7: Eq. (15) with the constraint (16) is thus changed into an initial value problem.

Step 8: Further the system is solved employing Runge-Kutta method.

Table 1. Review of wall shear stress coefficients for varied n .

n	$-f''(0)$			$-g''(0)$		
	Ariel [4]	Hayat et al. [21]	Present study	Ariel [4]	Hayat et al. [21]	Present study
0	1	1	1	0	0	0
0.1	1.020260	1.020260	1.020259	0.066847	0.066847	0.066850
0.2	1.039495	1.039495	1.039491	0.148737	0.148737	0.148775
0.3	1.057955	1.057955	1.057965	0.243360	0.243359	0.243356
0.4	1.075788	1.075788	1.075787	0.349209	0.349209	0.349212
0.5	1.093095	1.088662	1.088658	0.465205	0.465205	0.465212
0.6	1.109947	1.109947	1.109941	0.590529	0.590529	0.590519
0.7	1.126398	1.126398	1.126396	0.724532	0.724532	0.724530
0.8	1.142489	1.142489	1.142488	0.866683	0.866683	0.866678
0.9	1.158254	1.158255	1.158255	1.016539	1.016540	1.016543
1.0	1.173721	1.173722	1.173721	1.173721	1.173722	1.173719

4. Results and discussion

The coupled non-linear boundary layer Eqs. (9-12) subjected to the boundary values (13) are numerically solved by shooting method. In this study, the behavioural aspects of momentum($f'(\eta)$ and $g'(\eta)$), energy distribution and species distributions for different significant parameters are portrayed in Figs. 2 - 11. Due to practical importance, the coupled wall shear stress, energy and species transfer rate are shown in Tables 1 - 4.

Table 1 shows the appraisal results obtained in the present study and those of Ariel [4] and Hayat et al. [21].The results are quite in good agreement with the published works when:

$$\beta \rightarrow \infty, Ec_x = Ec_y = 0, R = 0, M = 0, K = 0, c = 1.$$

For improving λ values, the nanoflow displacement rate reduces; this is due to raise in recreation time that is the element wants more time for response from perturbed structure to equilibrium structure (Fig. 2). The effect of linear and non-linear radiation on the nanoflow energy is presented in Fig. 3. Initially the nanoflow energy drops, but picks up in the ambient stream. It is convincing to see the energy transfer is more in linearized approximation of radiation.

From Fig. 4, it is noticed that the fluid energy falls for enhancing Nt . The nanoparticles is repelled away from the hot convective surface and attracted towards the cold surface due to this thermos-diffusion act.

Pedesisimpact on the energy transfer and volume fraction dispersion is delineated in Figs. 5-6. It is perceived that the temperature rises near the wall and then falls far from surface as Nb enhances.

Due to convection swap, the nanoflow energy diminishes as the thermal Biot number improves (Fig. 7). Linearized radiation dominates initially then non-linearized approximated radiation pronounces in the quiescent flow.

Figs. 8-9 depict the influence of internal friction on the energy along axial and tangential direction. Both figures explain that the fluid temperature rises as the internal fluid friction

increases. Energy inside the fluid drops faster from the sheet in non-linearized diffusion approximation.

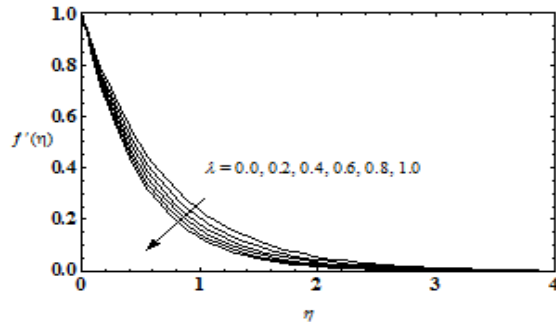


Fig. 2. Momentum profiles for λ .

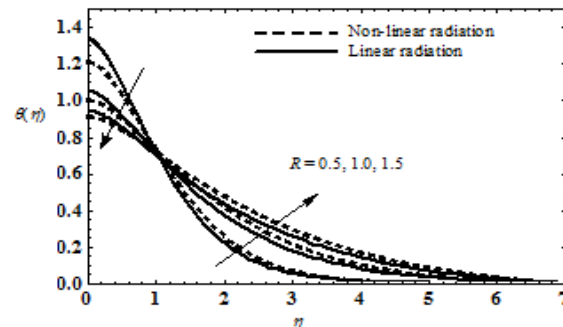


Fig. 3. Radiation effect on flow energy.

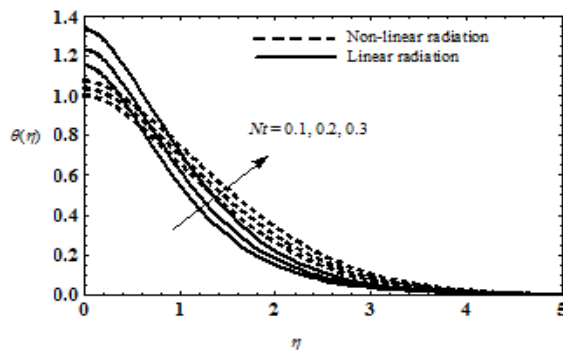


Fig. 4. Temperature for various on Nt .

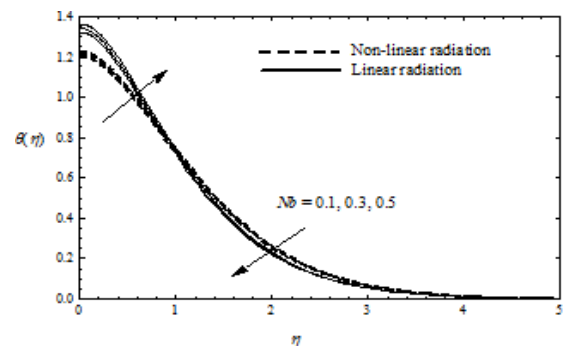


Fig. 5. Temperature profiles for varied Nb .

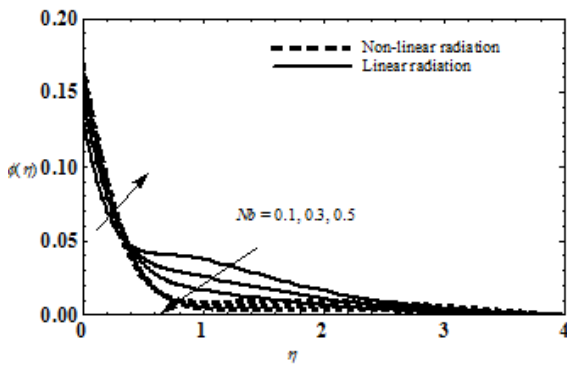


Fig. 6. Temperature profiles for varied Nb .

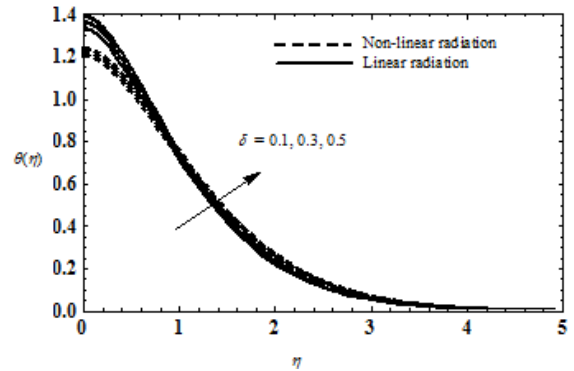


Fig. 10. Thermal Biot number influence on $\theta(\eta)$.

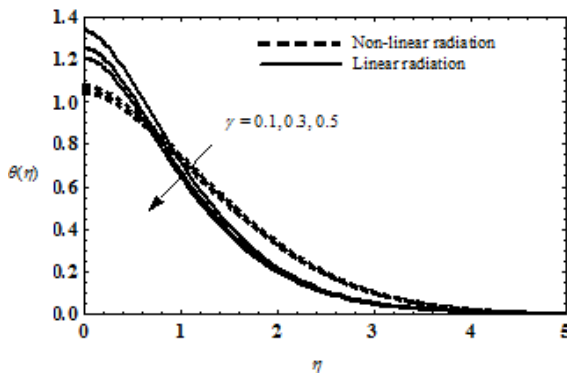


Fig. 7. Impact of γ on $\theta(\eta)$.

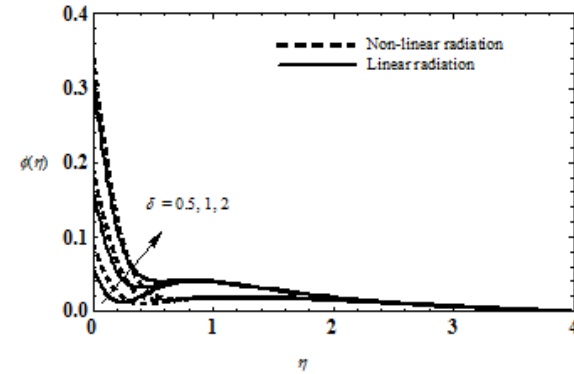


Fig. 11. Thermal Biot number impact on $\phi(\eta)$

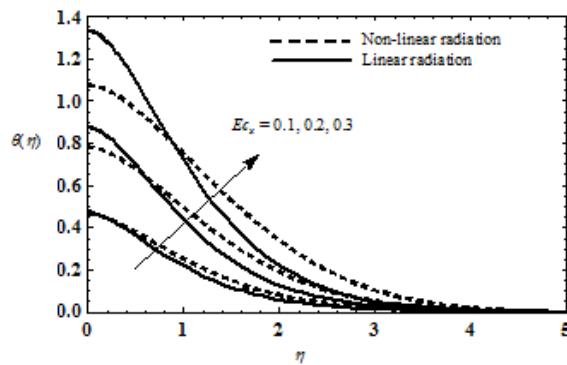


Fig. 8. Ec_x effect on nanoflow energy.

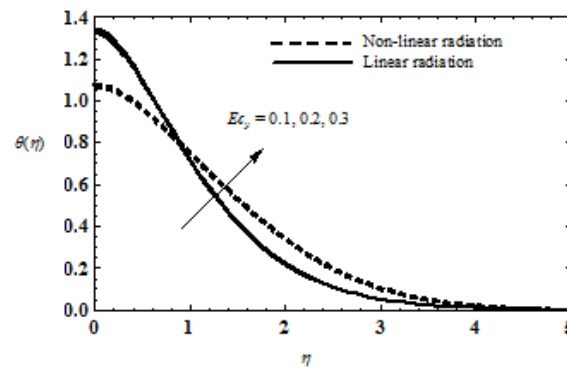


Fig. 9. Energy profiles for different Ec_y .

Solutal Biot number finds noticeable impression on the nanoflow energy and volume fraction (Figs. 10- 11).

Table 2, illustrates the variations of shear stress near the wall towards x and y -directions for different pertinent parameters. It is seen that the shear stress near wall descends when Jeffrey fluid parameter or magnetic field or stretch ratio ascend.

From Table 3, it is noted that the energy transmission rate weakens for augmenting Pr and also interestingly, it is seen that energy transmission is dominant in non-linearized radiation approximation. Eckert number the transmission rate of energy near the surface. Magnetic field diminishes the energy transmission rate as the resistance force acts in the reverse direction of the flow.

Enhancing Pedesis and thermophoresis parameter decreases heat transfer rate. Temperature gradient at the wall rises with a rise in thermal Biot number. In all the cases, it

is evident that nonlinear radiation transmits more energy.

From Table 4, it is noted that diffusion transfer rate is more when species Biot number increases. The same behaviour is noticed in Soret number case. Brownian movement

reduces the diffusion of species concentration transfer. Physically the random movement of the nanoparticles reduces the base fluid viscosity, so the diffusion rate of nanoparticles decreases.

Table 2. Evaluations of wall shear stresses.

λ	C	$f''(0)$	$g''(0)$
0.1	0.5	-1.36173	-0.610273
0.5		-1.59011	-0.712609
1.0		-1.83609	-0.822841
	0.1	-1.51883	-0.118736
	0.3	-1.55516	-0.393653
	0.5	-1.59011	-0.712609

Table 3. Computation of energy transfer rate.

Pr	R	Ec_x	Ec_y	Nt	Nb	γ	$-\theta'(0)$	
							Linear	Non-linear
0.71	0.5	0.3	0.3	0.3	0.3	0.1	0.018369	0.028579
1.00							0.042109	0.046531
2.00							0.058466	0.059613
0.71	1.0						0.042109	0.046531
	2.0						0.058466	0.059612
	3.0						0.064952	0.065039
	0.5	0.1					0.065192	0.065194
		0.2					0.042291	0.046029
		0.5					0.005993	0.020435
		0.3	0.1				0.018797	0.028873
			0.2				0.018583	0.028726
			0.5				0.017939	0.028287
			0.3	0.1			0.022772	0.030794
				0.2			0.020654	0.029699
				0.5			0.013199	0.026268
				0.3	0.1		0.019923	0.029321
					0.2		0.019151	0.028951
					0.5		0.016778	0.027839
					0.3	0.2	0.032005	0.048776
						0.3	0.042498	0.063574
						0.5	0.057541	0.083521

Table 4. Computations of Sherwood number for characterized flow parameters.

δ	Nt	Nb	Le	$-\phi'(0)$
0.1	0.3	0.3	5	0.107751
0.5				0.438077
1.0				0.710384
0.3	0.1			0.264024
	0.2			0.276511
	0.5			0.320215
	0.3	0.1		0.362555
		0.2		0.308081
		0.5		0.275412
			1	0.292183
			3	0.289016
			10	0.291963

5. Conclusions

The influence of Ohmic heating on MHD dissipating and radiating Jeffrey nanoflow past an extending sheet under Newtonian heat and mass flux constraints is investigated in this article. The outcomes was achieved by numerical techniques ; and the concluding remarks of the paper are

- Non-linear radiation transfers more energy from the fluid than linear.
- Shear stress along both directions descends for increasing flow parameter.
- Jeffrey fluid has greater stress relaxation property.
- Ascending magnetic parameter descends the wall shear stress.
- Stretching ratio parameter decreases the coefficient of wall shear stress.
- Energy transmission rate decreases as the internal friction (Ec) of the nanoflow enhances.
- SolutalBiot number and thermophoresis parameter increase the mass transfer rate while the Sherwood number decreases for improving Brownian motion and Lewis number.

References

- [1] P. Sreenivasulu, T. Poornima, B. Malleswari, N Bhaskar Reddy and BasmaSouayah, “Internal energy activation stimulus on magneto-bioconvective Powell-Eyringnanofluid containing gyrotactic microorganisms under active/passive nanoparticles flux”, *Phys. Scr.*, Vol. 96, No. 5, pp. 055221,(2021).
- [2] O. Ojjela, A. Raju and N. Naresh Kumar, “Influence of induced magnetic field and radiation on free convective Jeffrey fluid flow between two parallel porous plates with Soret and Dufour effects”, *J. Mech.*, Vol. 35, No. 5, pp. 657-675,(2019).
- [3] M. Kahshan, D. Lu and A. M. A. Siddiqui, “Jeffrey fluid model for a porous-walled channel: application to flat plate dialyzer”, *Sci. Rep.*, Vol. 9, 15879, (2019).
- [4] P. Donald Ariel, “Three-dimensional flow past a stretching sheet and the homotopy perturbation method”, *Comput. Math. Appl.*, Vol. 54, No. 7-8, pp. 920–925, (2007).
- [5] F. Mabood and K. Das, “Outlining the impact of melting on MHD Casson fluid flow past a stretching sheet in a porous medium with radiation”, *Heliyon*, Vol. 5, No. 2, pp.e01216,(2019).
- [6] B. Hussain, G. Janardhana Reddy, Abhishek, K. Annapoorna, V. Pujari, and N. Naresh Kumar, “Numerical modelling of second grade fluid flow past a stretching sheet”, *Heat transf. Asian Res.*, Vol. 48, No. 5, pp.1595-162, (2019).
- [7] J. Singh, U. S. Mahabaleshwar and Gabriella Bognár, “ Mass transpiration in nonlinear MHD flow due to porous stretching sheet”, *Sci. Rep.* ,Vol. 9, pp. 18484, (2019)
- [8] I. M. Alarifi, Ahmed G. Abokhalil, M. Osman, L. Ali Lund, M. Ben Ayed, H. Belmabrouk and I. Tlili, “MHD flow and heat transfer over vertical stretching sheet with heat sink or source effect”, *Symmetry*, Vol. 11, No. 297, pp. 1-24, (2019).
- [9] N. Kurikiyimfura, Y. Wang and Z. Pan, “Heat transfer enhancement by magnetic nanofluids-A review”, *Renew. Sustain. Energy Rev.*, Vol. 21, pp. 548-561, (2013).
- [10] M. Ferdows, M. S. Khan, O. A. Bég, M. Azad and M. MAlam, “Numerical study of transient magnetohydrodynamic radiative free convection nanofluid flow from a stretching permeable surface”, *Pi. Mech. Eng. E-J Pro.*, Vol. 228, No. 3, pp. 181-196, (2014).
- [11] M. Mustafa and J. Khan, “Model for flow of Casson nanofluid past a n on-linearly stretching sheet considering magnetic field effects”, *AIP Adv.*, Vol. 5, No. 7, pp. 077148, (2015).
- [12] V. P. Gohil and R. Meher, “Effect of magnetic field on imbibition phenomenon in the fluid flow through fractured porous media with different porous materials”,

- Nonlinear Eng.*, Vol. 8, No. 1, pp. 368–379, (2019).
- [13] M. Ramzan, M. Mutaz Mohammad and Fares Howari, “Magnetized suspended carbon nanotubes based nanofluid flow with bio-convection and entropy generation past a vertical cone”, *Sci. Rep.*, Vol. 9, pp. 12225, (2019).
- [14] P. Sreenivasulu, T. Poornima, B. Vasu, R. S. R. Gorla and N. Bhaskar Reddy, “Non-linear radiation and Navier-slip effects on UCM nanofluid flow past a stretching sheet under Lorentzian force”, *J. Appl. Comput. Mech.*, Vol. 7, No. 2, pp. 638-645, (2021).
- [15] M. Ali Abbas, M. Mubashir Bhatti and M. Sheikholeslami, “Peristaltic propulsion of Jeffrey nanofluid with thermal radiation and chemical reaction effects”, *Invent.*, Vol. 4, No. 4, pp. 1-16, (2019).
- [16] A. Hussain, L. Sarwar, S. Akbar, S. Nadeem and S. Jamal, “Numerical investigation of viscoelastic nanofluid flow with radiation effects”, *Proceed. Ins. Mech. Eng., Part N: J. Nanomater. Nanoeng. Nanosyst.*, Vol. 233, No. 2-4, pp. 87–96, (2019).
- [17] M. Sharma, R. Gaur and B. Kumar Sharma, “Radiation effect on MHD blood flow through a tapered porous stenosed artery with thermal and mass diffusion”, *Int. J. Appl. Mech. Eng.*, Vol. 24, No. 2, pp. 411-423, (2019).
- [18] M. Khan, M. Irfan and W. A. Khan, “Impact of nonlinear thermal radiation and gyrotactic microorganisms on the Magneto-Burgers nanofluid”, *Int. J. Mech. Sci.*, Vol. 130, pp. 375-382, (2017).
- [19] B. Souayeh, M. Gnanaswara Reddy, P. Sreenivasulu, T. Poornima, M. Rahimi-Gorji and I. M. Alarif, “Comparative analysis on non-linear radiative heat transfer on MHD Casson nanofluid past a thin needle”, *J. Mol. Liq.*, Vol. 284, pp. 163-174, (2019).
- [20] M. Gnanaswara Reddy and M. Ferdows, “Species and thermal radiation on micropolar hydro-magnetic dusty fluid flow across a paraboloid revolution”, *J. Therm. Anal. Calorim.*, Vol. 143, pp. 3699–3717, (2021).
- [21] T. Hayat, S. A. Shehzad and A. Alsaedi, “Three-dimensional stretched flow of Jeffrey fluid with variable thermal conductivity and thermal radiation”, *Appl. Math. Mech.*, Vol. 34, No. 7, pp. 823–832, (2013).
- [22] M. K. Nayak, S. Shaw, V. S. Pandey and A. J. Chamkha, “Combined effects of slip and convective boundary condition on MHD 3D stretched flow of nanofluid through porous media inspired by non-linear thermal radiation”, *Indian J. Phys.*, Vol. 92, No. 8, pp. 1017–1028, (2018).
- [23] S. Q. Chan, F. Aman and S. Mansur, “Bio-nanofluid flow through a moving surface adapting convective boundary condition: sensitivity”, *J. Adv. Res. Fluid Mech. Therm. Sci.*, Vol. 54, No. 1, pp. 57-69, (2019).
- [24] H. C. Brinkman, “Heat effects in capillary flow”, *Appl. Sci. Res.*, Vol. 2, pp. 120-124, (1951).
- [25] J. A. Fillo, “Viscous and Joule heating effects on the heat transfer from a flat plate”, *Phys. Fluids.*, Vol. 11, No. 2, pp. 437, (1968).
- [26] A. Hussain, M. Y. Malik, T. Salahuddin, S. Bilal and M. Awais, “Combined effects of viscous dissipation and Joule heating on MHD Sisko nanofluid over a stretching cylinder”, *J. Mol. Liq.*, Vol. 231, pp. 341-352, (2017).
- [27] Md. Shamsuddin and P. V. SatyaNarayana, “Combined effect of viscous dissipation and Joule heating on MHD flow past a Riga plate with Cattaneo–Christov heat flux”, *Indian J. Phys.*, Vol. 94, pp. 1385-1394, (2020).
- [28] T. Hayat, A. Aziz, T. Muhammad and A. Alsaedi, “Three-dimensional flow of nanofluid with heat and mass flux boundary conditions”, *Chin. J. Phys.*, Vol. 55, No. 4, pp. 1495-1510, (2017).

Copyrights ©2021 The author(s). This is an open access article distributed under the terms of the Creative Commons Attribution (CC BY 4.0), which permits unrestricted use, distribution, and reproduction in any medium, as long as the original authors and source are cited. No permission is required from the authors or the publishers.



How to cite this paper:

B. Malliswari, T. Poornima, P. Sreenivasulu and N. Bhaskar Reddy, “Electrical resistance heating distribution on three dimensional Jeffrey radiating nanofluid flow past stretching surface,” *J. Comput. Appl. Res. Mech. Eng.*, Vol. 11, No. 2, pp. 339-349, (2022).

DOI: 10.22061/JCARME.2021.7013.1908

URL: https://jcarme.sru.ac.ir/?_action=showPDF&article=1569

